Geometry of classical periodic orbits and quantum coherent states in coupled oscillators with SU(2) transformations

Y. F. Chen[*]

Department of Electrophysics, National Chiao Tung University, 1001 Ta-Huseh Road, Hsinchu 30050, Taiwan

The geometry of classical dynamics in coupled oscillators with SU(2) transformations is explored and found to be relevant to a family of continuous-transformation orbits between Lissajous and trochoidal curves. The quantum wave-packet coherent states are derived analytically to correspond exactly to the transformation geometry of classical dynamics. By using the quantum wave-packet coherent states derived herein, stationary coherent states are constructed and are shown to possess spatial patterns identical to the transformation geometry between Lissajous and trochoidal orbits.

I. INTRODUCTION

Recently, much research on quantum physics has revealed that quantum wave functions correlated with classical periodic orbits play a critical role in explaining striking quantum phenomena such as shell effects in nuclei and metallic clusters [1,2], conductance fluctuations in mesoscopic semiconductor billiards [3,4], and oscillations in photodetachment cross sections [5,6]. Explicitly, quantum wave functions localized on classical orbits emerge quite naturally and inevitably in the quantum-classical transition. Quantum wave-packet coherent states [7,8] have been verified to be not only the most representative states related to classical dynamics but also the most [1] persistent states in the system interacting with the environment [9]. Therefore, quantum coherent states localized on classical orbits have been explored in different branches of physics such as solid-state, nuclear, and atomic physics [10–13].

Modern laser cavities have been employed extensively to serve as an analogous system to provide an experimental visualization in an optical context to confirm many quantum effects such as quantum chaos phenomena [14,15], disorder-induced wave localization [16], geometric phases [17], and quantum tunneling [18]. Spatial structures of laser modes in broad-area resonators have been of interest for a long time because they offer much insight into the pattern formation of natural waves [19–27]. More recently, wave patterns of high-order coherent laser modes in various cavities have been generated to manifest the morphologies of quantum coherent states related to periodic orbits [28–30]. The most remarkable finding is that the coherent optical waves related to the Lissajous and trochoidal patterns can be geometrically connected through SU(2) transformations [31]. The geometric connection in coherent optics signifies the relevance of exploring the transformation geometry of quantum coherent states in the quantum-classical correspondence. Nevertheless, to the best of the author's knowledge, there have been no systematic investigations involving the transformation geometry of quantum coherent states.

The two-dimensional (2D) coupled harmonic oscillator is an important model used to describe various physical properties such as bosonic realization of SU(2) Lie algebra [32], generation and evolution of quantum vortex states [33,34], orbital magnetism in quantum dots [35], charged particles in external fields [36,37], and shell effects in nuclei and metallic clusters [38]. In this paper the transformation geometry of classical dynamics in the 2D coupled harmonic oscillator related to SU(2) transformations is investigated. The classical periodic orbits under SU(2) transformations are found to exhibit a family of continuous transformation orbits between Lissajous and trochoidal curves. Quantum wave-packet coherent states corresponding to the transformation geometry of classical dynamics are derived. These quantum wave-packet coherent states are exploited to extract stationary coherent states with spatial morphologies concentrated on the transformation geometry. Since the quantum coherent states related to the SU(2) transformation geometry generally carry angular momenta [1], the present investigation should be helpful in generating coherent optical waves with spatial structures for many applications.

II. GENERALIZED HAMILTONIAN RELATED TO SU(2) TRANSFORMATIONS

By using the dimensionless spatial variables $\tilde{x}$ and $\tilde{y}$, the Hamiltonian for the 2D isotropic oscillator is given by

$$\hat{H}_0 = \frac{\omega_0}{2}\left(\tilde{p}_x^2 + \tilde{p}_y^2 + \tilde{x}^2 + \tilde{y}^2\right). \tag{1}$$

In terms of the ladder operators, the quantum Hamiltonian becomes $\hat{H}_0 = (\hat{a}_1^\dagger \hat{a}_1 + \hat{a}_2^\dagger \hat{a}_2 + 1)\omega_0$, where $\hat{a}_1 = (\tilde{x} + i\tilde{p}_x)/\sqrt{2}$, $\hat{a}_1^\dagger = (\tilde{x} - i\tilde{p}_x)/\sqrt{2}$, $\hat{a}_2 = (\tilde{y} + i\tilde{p}_y)/\sqrt{2}$, and $a_2^\dagger = (\tilde{y} - i\tilde{p}_y)/\sqrt{2}$. Note that $\hbar = 1$ has been chosen for the units. The generalized Hamiltonian related to SU(2) transformations for the coupled oscillator systems can be modeled as

$$\hat{H} = \hat{H}_0 + \sum_{i=1}^{3} \Omega_i \hat{L}_i, \tag{2}$$

where the coupling parameters Ω_i are assumed to be real constants and the operators $\hat{L}_1 = 1/2(\hat{a}_1^\dagger \hat{a}_2 + \hat{a}_2^\dagger \hat{a}_1)$, $\hat{L}_2 = -i/2(\hat{a}_1^\dagger \hat{a}_2 - \hat{a}_2^\dagger \hat{a}_1)$, and $\hat{L}_3 = 1/2(\hat{a}_1^\dagger \hat{a}_1 - \hat{a}_2^\dagger \hat{a}_2)$ are derived by Schwinger [39] to discuss the correspondence between two linear oscillators and an angular momentum oscillator. The

---

*yfchen@cc.nctu.edu.tw

operators $\hat{L}_i$ satisfy the usual angular momentum commutation relations, i.e., Lie commutator algebra $[\hat{L}_i, \hat{L}_j] = i\varepsilon_{i,j,k}\hat{L}_k$, where the Levi-Civita tensor $\varepsilon_{i,j,k}$ is equal to $+1$ and -1 for even and odd permutations of its indices, respectively, and zero otherwise. The Hamiltonian in Eq. (2) can represent a host of entanglement mechanisms [40–42] and can be used to analyze a single laser-cooled ion confined in a harmonic trap [43]. In wave optics, the operators $\hat{L}_1$, $\hat{L}_2$, and $\hat{L}_3$ are associated with astigmatism and aberration [44]. Consequently, the present investigation is also relevant in high-order laser pattern formations [45].

First we analyze the classical dynamics for the Hamiltonian $\hat{H}$ to acquire background information to study the quantum wave-packet coherent states. By using the dimensionless spatial variables, the operators $\hat{L}_1$, $\hat{L}_2$, and $\hat{L}_3$ can be expressed as $\hat{L}_1 = 1/2(\tilde{x}\tilde{y} + \tilde{p}_x\tilde{p}_y)$, $\hat{L}_2 = 1/2(\tilde{x}\tilde{p}_y - \tilde{y}\tilde{p}_x)$, and $\hat{L}_3 = 1/4(\tilde{x}^2 + \tilde{p}_x^2 - \tilde{y}^2 - \tilde{p}_y^2)$. The classical equation of motion for the Hamiltonian $\hat{H}$ is

$$i\frac{d}{dt}\begin{bmatrix} \upsilon_1 \\ \upsilon_2 \end{bmatrix} = \begin{bmatrix} \omega_0 + (\Omega_3/2) & (\Omega_1 - i\Omega_2)/2 \\ (\Omega_1 + i\Omega_2)/2 & \omega_0 - (\Omega_3/2) \end{bmatrix}\begin{bmatrix} \upsilon_1 \\ \upsilon_2 \end{bmatrix}, \quad (3)$$

where $\upsilon_1 = \tilde{x} + i\tilde{p}_x$ and $\upsilon_2 = \tilde{y} + i\tilde{p}_y$. Even though Eq. (3) is the equation of motion for $\hat{H}$ in classical mechanics, its form is the same as the Schrödinger equation for a two-level system, e.g., spinor states in a magnetic field. By using

the SU(2) algebra, the general solution for Eq. (3) can be solved as

$$\begin{bmatrix} \upsilon_1(t) \\ \upsilon_2(t) \end{bmatrix} = \begin{bmatrix} e^{-i\alpha/2}\cos(\beta/2) & -e^{-i\alpha/2}\sin(\beta/2) \\ e^{i\alpha/2}\sin(\beta/2) & e^{i\alpha/2}\cos(\beta/2) \end{bmatrix}\begin{bmatrix} \mu_1(t) \\ \mu_2(t) \end{bmatrix},$$

(4)

where $\alpha = \tan^{-1}(\Omega_2/\Omega_1)$, $\beta = \tan^{-1}(\sqrt{\Omega_1^2 + \Omega_2^2}/\Omega_3)$, $\mu_1(t) = A_1 e^{-i(\omega_1 t - \phi_1)}$, $\mu_2(t) = A_2 e^{-i(\omega_2 t - \phi_2)}$, $\omega_1 = \omega_0 + (\Omega/2)$, $\omega_2 = \omega_0 - (\Omega/2)$, $\Omega = \sqrt{\Omega_1^2 + \Omega_2^2 + \Omega_3^2}$, and A_1, A_2, ϕ_1, and ϕ_2 are related to the initial conditions. Consequently, the generalized classical orbits for $\hat{H}$ are given by

$$\begin{aligned} \tilde{x}(t) &= A_1\cos(\beta/2)\cos(\omega_1 t - \phi_1 - \alpha/2) \\ &\quad - A_2\sin(\beta/2)\cos(\omega_2 t - \phi_2 - \alpha/2), \\ \tilde{y}(t) &= A_1\sin(\beta/2)\cos(\omega_1 t - \phi_1 \\ &\quad + \alpha/2) + A_2\cos(\beta/2)\cos(\omega_2 t - \phi_2 + \alpha/2). \end{aligned} \quad (5)$$

The orbits in Eq. (5) are particularly well known for several values of α and β. For example, the parametric equations for $\alpha = 0$ are given by

$$\begin{aligned} \tilde{x}(t) &= A_1\cos(\beta/2)\cos(\omega_1 t - \phi_1) \\ &\quad - A_2\sin(\beta/2)\cos(\omega_2 t - \phi_2), \\ \tilde{y}(t) &= A_1\sin(\beta/2)\cos(\omega_1 t - \phi_1) \\ &\quad + A_2\cos(\beta/2)\cos(\omega_2 t - \phi_2). \end{aligned} \quad (6)$$

The family of curves in Eq. (6) is represented by Lissajous figures at an angle of $\beta/2$ with respect to the x axis. Figure 1
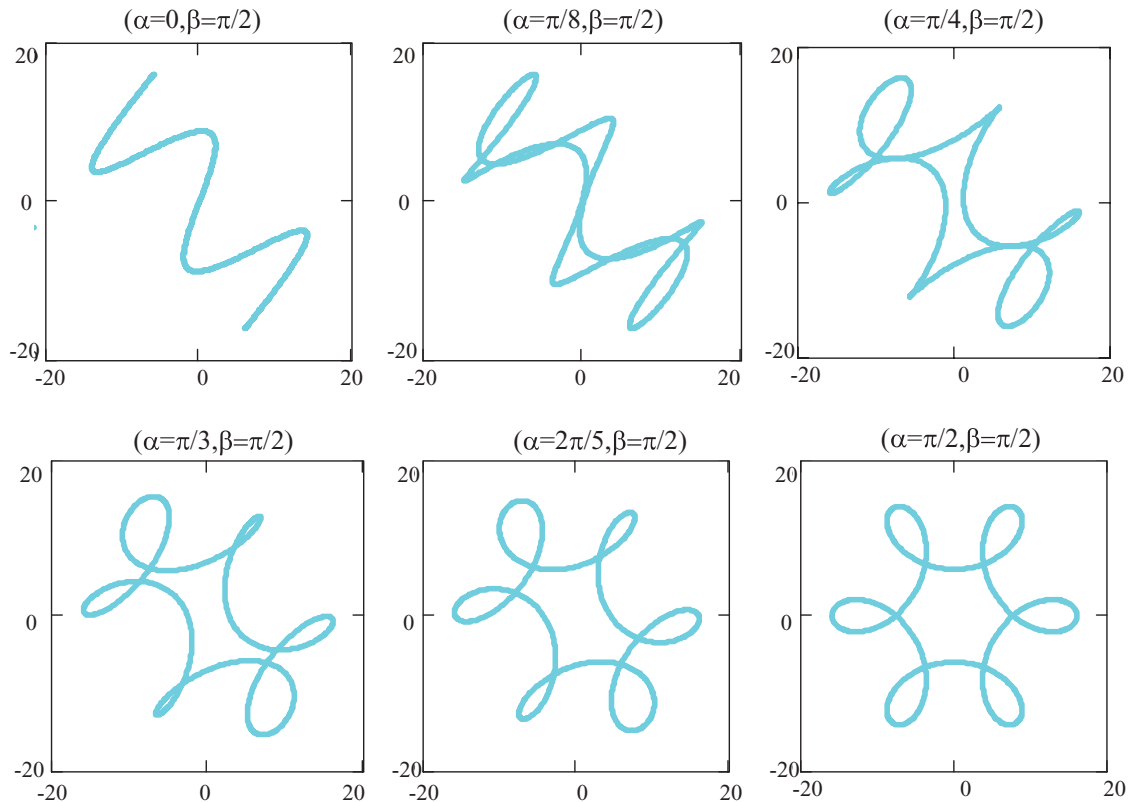

FIG. 1. (Color online) Periodic orbits for the case of $\omega_1\omega_2 = 5/1$ for various values of α for the parameters $(A_1, A_2) = (25, 120)$, $\phi_1 = \phi_2 = 0$, and $\beta = \pi/2$ in Eq. (5).
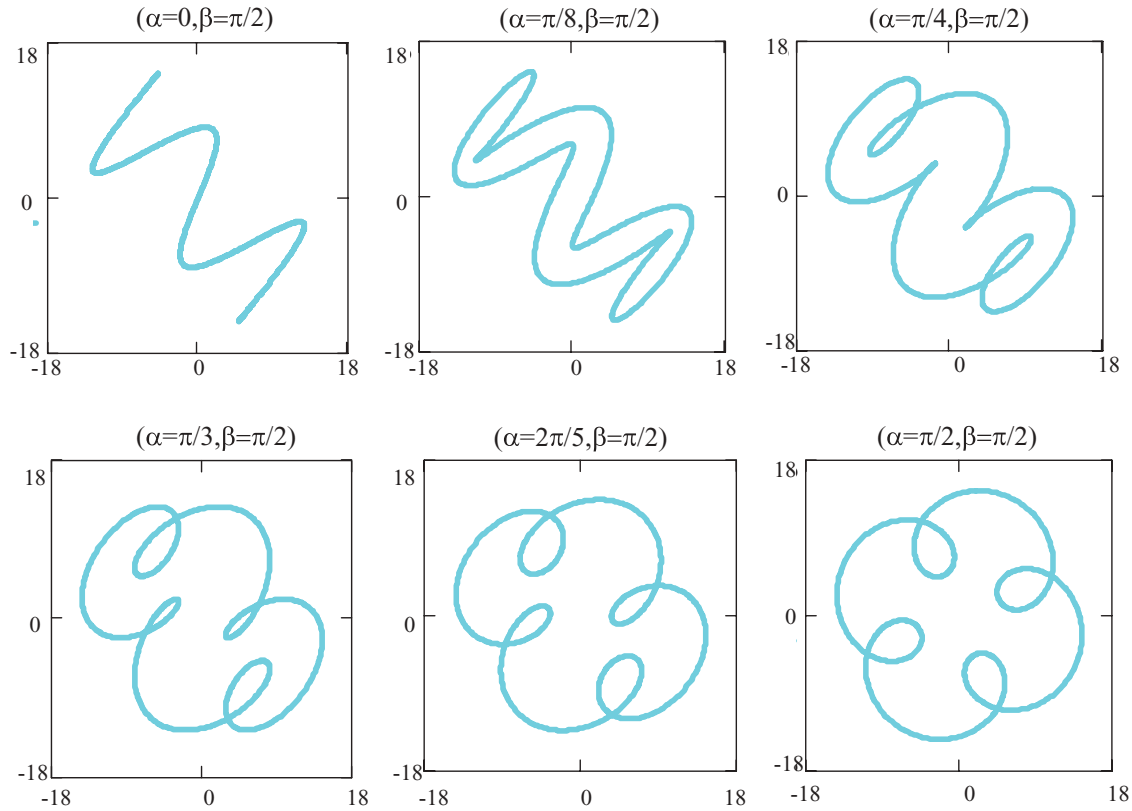
FIG. 2. (Color online) Periodic orbits for the case of $\omega_1/\omega_2 = -5/1$ for various values of α for the parameters $(A_1, A_2) = (25, 100)$, $\phi_1 = \phi_2 = 0$, and $\beta = \pi/2$ in Eq. (5).

depicts the periodic orbits for the case of $\omega_1/\omega_2 = 5/1$ for various values of α for the parameters $(A_1, A_2) = (25, 120)$, $\phi_1 = \phi_2 = 0$, and $\beta = \pi/2$ in Eq. (5). It can be seen that the orbits are associated with a continuous transformation between Lissajous figures and hypotrochoids for different values of the parameter α. In contrast, Fig. 2 shows the periodic orbits for the case of $\omega_1/\omega_2 = -5/1$ for various values of α for the parameters $(A_1, A_2) = (25, 100)$, $\phi_1 = \phi_2 = 0$, and $\beta = \pi/2$ in Eq. (5). In this case, the orbits are found to be a continuous transformation between Lissajous figures and epitrochoids for various values of the parameter α. In brief, the orbit in Eq. (5) for $\alpha = \pi/2$ and $\beta = \pi/2$ can be a hypotrochoid or an epitrochoid, depending on whether the ratio ω_1/ω_2 is positive or negative. Mathematically, a hypotrochoid (epitrochoid) is a roulette [1] traced by a point attached to a circle at a point other than the center when the circle rolls without slipping on the inside (outside) of a fixed circle. Note that a hypocycloid (epicycloid) is a hypotrochoid (epitrochoid) for which the tracing point is precisely on the circumference of the rolling circle. To sum up, by using SU(2) transformations the classical dynamics of the coupled oscillator in Eq. (2) are shown to display a wide variety of curves, which are given in Eq. (5). For convenience these curves are called Lissajous-trochoid transformed curves since these curves are associated with a continuous transformation between Lissajous figures and trochoids for various values of the parameters α and β in Eq. (5). Note that the Lissajous-trochoid orbits are invariant with respect to changes in the phases ϕ_1 and ϕ_2 provided the quantity $\gamma = p\phi_1 \mp q\phi_2$ remains [1] modulo 2π.

III. WAVE-PACKET COHERENT STATES RELATED TO SU(2) TRANSFORMATIONS

The eigenstates of $\hat{H}_0$ are the two-mode Fock state $|n_1, n_2\rangle_{\hat{H}_0} = [(\hat{a}_1^\dagger)^{n_1}/\sqrt{n_1!}] [(\hat{a}_2^\dagger)^{n_2}/\sqrt{n_2!}]|0,0\rangle_{\hat{H}_0}$ and their eigenvalues are $E_{\hat{H}_0}(n_1, n_2) = (n_1 + n_2 + 1)\omega_0$, where n_1 and n_2 are positive integers and $|0,0\rangle_{\hat{H}_0}$ represents the ground state. The normalized spatial representation is given by

$$\langle \tilde{x}, \tilde{y} | n_1, n_2 \rangle_{\hat{H}_0} = [2^{n_1+n_2}(n_1!)(n_2!)\pi]^{-1/2}$$
$$e^{-(\tilde{x}^2+\tilde{y}^2)/2} H_{n_1}(\tilde{x}) H_{n_2}(\tilde{y}), \quad (7)$$

where $H_n(\tilde{x})$ are the Hermite polynomials. To find the eigenstates of the coupled oscillator $\hat{H}$ in Eq. (2) we employ the same SU(2) algebra for classical dynamics to define a new pair of operators

$$\begin{bmatrix} \hat{a}'_1 \\ \hat{a}'_2 \end{bmatrix} = \begin{bmatrix} e^{i\alpha/2}\cos(\beta/2) & e^{-i\alpha/2}\sin(\beta/2) \\ -e^{i\alpha/2}\sin(\beta/2) & e^{-i\alpha/2}\cos(\beta/2) \end{bmatrix} \begin{bmatrix} \hat{a}_1 \\ \hat{a}_2 \end{bmatrix}. \quad (8)$$

By using the operators $\hat{a}'_1$ and $\hat{a}'_2$ in Eq. (8), the coupled oscillator $\hat{H}$ in Eq. (2) can be transformed into a separable 2D harmonic oscillator:

$$\hat{H} = (\hat{a}'^\dagger_1 \hat{a}'_1 + \tfrac{1}{2})\omega_1 + (\hat{a}'^\dagger_2 \hat{a}'_2 + \tfrac{1}{2})\omega_2. \quad (9)$$

As a result, the eigenstates and eigenvalues of the Hamiltonian $\hat{H}$ can be found to be $|n_1, n_2\rangle_{\hat{H}} = [(\hat{a}'^\dagger_1)^{n_1}/\sqrt{n_1!}] [(\hat{a}'^\dagger_2)^{n_2}/\sqrt{n_2!}]|0,0\rangle_{\hat{H}}$ and $E_{\hat{H}}(n_1, n_2) = (n_1 + 1/2)\omega_1 + (n_2 + 1/2)\omega_2$, respectively. Note that $|0,0\rangle_{\hat{H}} = |0,0\rangle_{\hat{H}_0}$. In terms of the Wigner d-matrix elements,

the eigenstates $|n_1,n_2\rangle_{\hat{H}}$ can be explicitly expressed as a linear combination of the eigenstates of the uncoupled oscillator:

$$|n_1,n_2\rangle_{\hat{H}} = e^{iN\alpha/2} \sum_{m_1=0}^{N} e^{-im_1\alpha} d_{m_1-N/2,n_1-N/2}^{N/2}(\beta)|m_1,m_2\rangle_{\hat{H}_0}, \tag{10}$$

where $N = n_1 + n_2 = m_1 + m_2$ and

$$d_{m_1-N/2,n_1-N/2}^{N/2}(\beta)$$
$$= \sqrt{m_1!(N-m_1)!n_1!(N-n_1)!} \sum_{\nu=\max[0,m_1-n_1]}^{\min[N-n_1,m_1]}$$
$$\times \frac{(-1)^{\nu}[\cos(\beta/2)]^{N-n_1+m_1-2\nu}[\sin(\beta/2)]^{n_1-m_1+2\nu}}{\nu!(N-n_1-\nu)!(m_1-\nu)!(n_1-m_1+\nu)!}. \tag{11}$$

The eigenstates in Eq. (10) do not directly correspond to the classical Lissajous-trochoid orbits; it is necessary to construct quantum wave-packet coherent states to mimic classical dynamics.

The quantum wave-packet states developed by Schrödinger for 1D harmonic oscillators are given by

$$|\Psi(t;\mu)\rangle = e^{-i\omega_0 t/2} \sum_{n=0}^{\infty} \frac{\mu^n}{n!} e^{-|\mu|^2/2}(\hat{a}^{\dagger})^n |0\rangle, \tag{12}$$

where $\mu = Ae^{-i(\omega_0 t-\phi)}$ and A and ϕ are related to the initial condition of the trajectory. By using the generating function of the Hermite polynomials, the probability distributions of the Schrödinger coherent states can be derived as

$$P(\tilde{x},t;\mu) = |\langle\tilde{x} \mid \Psi(t;\mu)\rangle|^2 = \frac{1}{\sqrt{\pi}} \exp\{-[\tilde{x}-\sqrt{2}\text{Re}(\mu)]^2\}. \tag{13}$$

Equation (13) indicates that the center of the coherent states moves in the path of the harmonic waves $\tilde{x}(t) = \sqrt{2}\text{Re}[\mu(t)] = \sqrt{2}A\cos(\omega t - \phi)$. The coupled oscillator $\hat{H}$ in Eq. (2) can be transformed into a separable 2D harmonic oscillator in terms of the operators $\hat{a}'_1$ and $\hat{a}'_2$ in Eq. (9). As a consequence, the quantum coherent states can be expressed as the product of two 1D coherent states:

$$|\Psi(t;\mu_1,\mu_2)\rangle = e^{-i(\omega_1+\omega_2)t/2} \sum_{n_1=0}^{\infty}$$
$$\times \sum_{n_2=0}^{\infty} e^{-(|\mu_1|^2+|\mu_2|^2)/2} \frac{\mu_1^{n_1}}{n_1!}\frac{\mu_2^{n_2}}{n_2!}(\hat{a}'_1{}^{\dagger})^{n_1}(\hat{a}'_2{}^{\dagger})^{n_2}|0,0\rangle_{\hat{H}}, \tag{14}$$

where $\mu_1(t) = A_1e^{-i(\omega_1 t-\phi_1)}$ and $\mu_2(t) = A_2e^{-i(\omega_2 t-\phi_2)}$. Substituting Eq. (8) into Eq. (14), after cumbersome algebra, Eq. (14) can be transformed into

$$|\Psi(t;\upsilon_1,\upsilon_2)\rangle = e^{-i\omega_0 t} \sum_{m_1=0}^{\infty}$$
$$\times \sum_{m_2=0}^{\infty} e^{-(|\upsilon_1|^2+|\upsilon_2|^2)/2} \frac{\upsilon_1^{m_1}}{m_1!}\frac{\upsilon_2^{m_2}}{m_2!}(\hat{a}_1^{\dagger})^{m_1}(\hat{a}_2^{\dagger})^{m_2}|0,0\rangle_{\hat{H}_0}, \tag{15}$$

where the relationship between $[\upsilon_1(t),\upsilon_2(t)]$ and $[\mu_1(t),\mu_2(t)]$ is exactly the same as in Eq. (4). By using the result in Eq. (13),

the probability distribution of the coherent state $|\Psi(t;\upsilon_1,\upsilon_2)\rangle$ is

$$P(\tilde{x},\tilde{y},t) = |\langle\tilde{x},\tilde{y} \mid \Psi(t;\upsilon_1,\upsilon_2)\rangle|^2$$
$$= \frac{1}{\pi} \exp(-\{\tilde{x}-\sqrt{2}\text{Re}[\upsilon_1(t)]\}^2)$$
$$\times \exp(-\{\tilde{y}-\sqrt{2}\text{Re}[\upsilon_2(t)]\}^2). \tag{16}$$

Equation (16) indicates that the probability distributions of the coherent states $|\Psi(t;\upsilon_1,\upsilon_2)\rangle$ are concentrated exactly on the Lissajous-trochoid transformed curves shown in Eq. (5).

IV. STATIONARY COHERENT STATES RELATED TO SU(2) TRANSFORMATIONS

Like quantum elliptical states of the Rydberg hydrogen atom [10], wave-packet coherent states $|\Psi(t;\upsilon_1,\upsilon_2)\rangle$ can be expressed as a superposition of stationary coherent states. The stationary coherent states are a coherent superposition of degenerate eigenstates. The wave pattern of the stationary coherent states is localized on the corresponding classical periodic orbits. As the number of quanta increases, the localization on the classical invariant structure is more prominent. These coherent states not only give a useful representation to which classical and quantum mechanics can be compared but also constitute a convenient basis in which to study weak perturbations. To derive a general expression for the stationary coherent state, we first simplify the wave-packet coherent state $|\Psi(t;\upsilon_1,\upsilon_2)\rangle$ as a double finite sum for sufficiently large values of A_1 and A_2 (say A_1 and $A_1 > 10$). From Eq. (15) the probability P_{n_1,n_2} of the coherent state $|\Psi(t;\upsilon_1,\upsilon_2)\rangle$ in an eigenstate $|n_1,n_2\rangle_{\hat{H}}$ can be found to be a 2D Poisson distribution:

$$P_{n_1,n_2} = \left(\frac{\bar{n}_1^{n_1}}{n_1!}e^{-\bar{n}_1}\right)\left(\frac{\bar{n}_2^{n_2}}{n_2!}e^{-\bar{n}_2}\right), \tag{17}$$

where the mean values of $\bar{n}_1$ and $\bar{n}_2$ are given by $\bar{n}_1 = \langle\Psi|\hat{a}_1'^{\dagger}\hat{a}_1'|\Psi\rangle = A_1^2$ and $\bar{n}_2 = \langle\Psi|\hat{a}_2'^{\dagger}\hat{a}_2'|\Psi\rangle = A_2^2$ [1], respectively. For the central limit theorem, the distribution P_{n_1,n_2} approaches a 2D Gaussian distribution with means $\bar{n}_1$ and $\bar{n}_2$ and standard deviations $\sqrt{\bar{n}_1}$ and $\sqrt{\bar{n}_2}$. Therefore, the coherent state $|\Psi(t;\upsilon_1,\upsilon_2)\rangle$ can be appropriately expressed as a double finite sum of the dominant [1] eigenstates:

$$|\Psi(t;\upsilon_1,\upsilon_2)\rangle = e^{-i\vartheta(t)}\left(\sum_{s_1=-[2\sqrt{\bar{n}_1}]}^{[2\sqrt{\bar{n}_1}]}\sum_{s_2=-[2\sqrt{\bar{n}_2}]}^{[2\sqrt{\bar{n}_2}]}\frac{e^{-is_1(\omega_1 t-\phi_1)}}{\sqrt{\sqrt{2\pi\bar{n}_1}}}\right.$$
$$\left.\times e^{-s_1^2/4\bar{n}_1}\frac{e^{-is_2(\omega_2 t-\phi_2)}}{\sqrt{\sqrt{2\pi\bar{n}_2}}}e^{-s_2^2/4\bar{n}_2}|\bar{n}_1+s_1,\bar{n}_2+s_2\rangle_{\hat{H}}\right), \tag{18}$$

where $e^{-i\vartheta(t)} = e^{-i(\omega_1+\omega_2)t/2}e^{-i\bar{n}_1(\omega_1 t-\phi_1)}e^{-i\bar{n}_2(\omega_2 t-\phi_2)}$ and $[w]$ is the Gaussian bracket (integer closest to w on the lower side). For convenience we set $\omega_1 = q\omega$ and $\omega_2 = \pm p\omega$, where p and q are prime [1], positive integers. For $\omega_1 = q\omega$ and $\omega_2 = \pm p\omega$, the set of states with indices (s_1,s_2) in Eq. (18) can be divided into subsets characterized by a pair of indices (u_1,u_2) given by
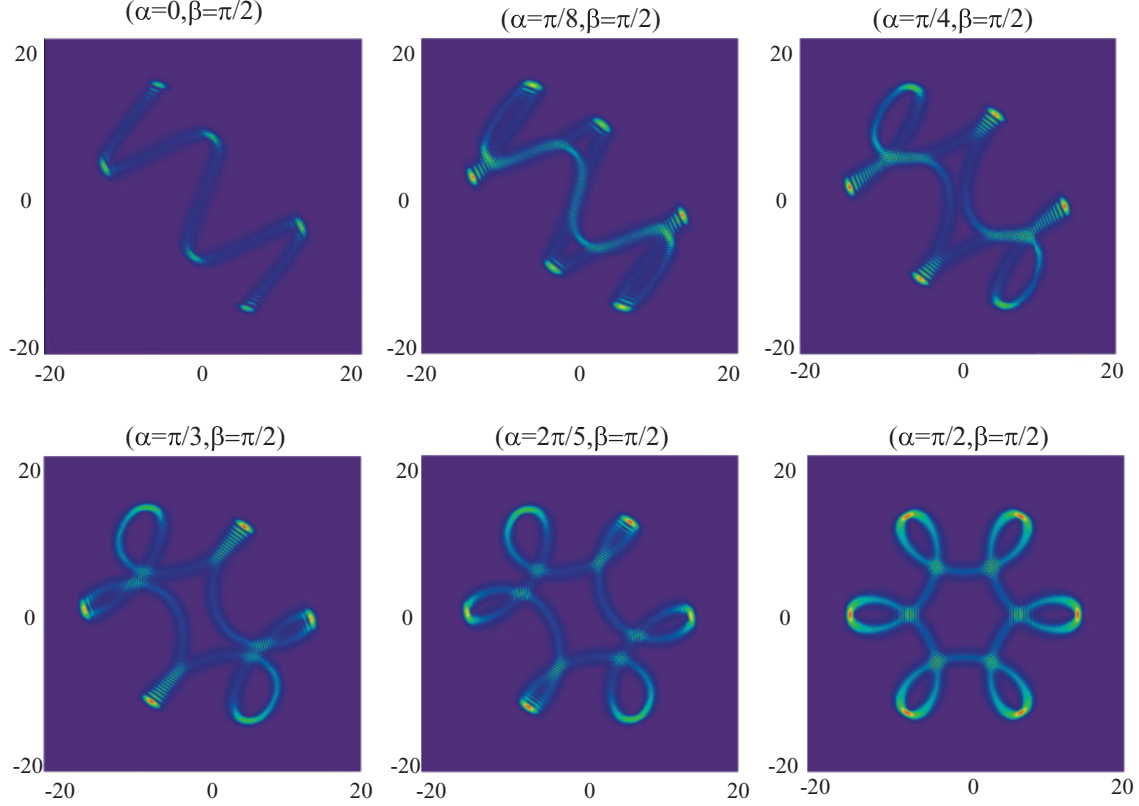
FIG. 3. (Color online) Wave patterns of the stationary coherent state $|\Psi_{\bar{n}_1,\bar{n}_2}^{\pm p,q}(\gamma)\rangle_{0,0,0}$ for the parameters corresponding to the classical orbits shown in Fig. 1.

$s_1 \equiv u_1 (\mathrm{mod}\, p)$ and $s_2 \equiv u_2 (\mathrm{mod}\, q)$. In terms of these subsets, we can rewrite the coherent state in Eq. (18) as

$$
|\Psi(t; \upsilon_1, \upsilon_2)\rangle = e^{-i\vartheta(t)} \Bigg(\sum_{u_1=0}^{p-1} e^{-iu_1(q\omega t - \phi_1)} \sum_{u_2=0}^{q-1} e^{-iu_2(\pm p\omega t - \phi_2)}
$$

$$
\times \sum_{k_1=-[2\sqrt{\bar{n}_1}/p]}^{[2\sqrt{\bar{n}_1}/p]} \sum_{k_2=-[2\sqrt{\bar{n}_2}/q]}^{[2\sqrt{\bar{n}_2}/q]} \frac{e^{-ipk_1(q\omega t - \phi_1)}}{\sqrt{\sqrt{2\pi\bar{n}_1}}}
$$

$$
\times e^{-[(pk_1+u_1)^2/4\bar{n}_1]} \frac{e^{-iqk_2(\pm p\omega t - \phi_2)}}{\sqrt{\sqrt{2\pi\bar{n}_2}}} e^{-[(qk_2+u_2)^2/4\bar{n}_2]}
$$

$$
\times |\bar{n}_1 + pk_1 + u_1, \bar{n}_2 + qk_2 + u_2\rangle_{\hat{H}} \Bigg). \tag{19}
$$

To extract the stationary coherent state, the indices k_1 and k_2 in Eq. (19) are replaced by the indices $k_1 = (s+k)/2$ and $k_2 = \pm(s-k)/2$, where the sign of the index k corresponds to the sign of $\omega_2 = \pm p\omega$. Consequently, the wave-packet coherent state in Eq. (19) can be given by

$$
|\Psi(t; \upsilon_1, \upsilon_2)\rangle = e^{-i\vartheta(t)} \sum_{u_1=0}^{p-1} e^{-iu_1(q\omega t - \phi_1)} \sum_{u_2=0}^{q-1} e^{-iu_2(\pm p\omega t - \phi_2)}
$$

$$
\times \sum_{s=-S}^{S} e^{-i2sp q\omega t} e^{is(p\phi_1 \pm q\phi_2)} |\Psi_{\bar{n}_1,\bar{n}_2}^{\pm p,q}(\gamma)\rangle_{s,u_1,u_2}, \tag{20}
$$

where $S = [2\sqrt{\bar{n}_1}p + 2\sqrt{\bar{n}_2}q]$ and the stationary coherent state $|\Psi_{\bar{n}_1,\bar{n}_2}^{\pm p,q}(\gamma)\rangle_{s,u_1,u_2}$ is given by

$$
|\Psi_{\bar{n}_1,\bar{n}_2}^{\pm p,q}(\gamma)\rangle_{s,u_1,u_2} = \frac{1}{\sqrt{2\pi\sqrt{\bar{n}_1\bar{n}_2}}}
$$

$$
\times \sum_{k=L(s)}^{U(s)} e^{ik\gamma} e^{-\{[p(s+k)+u_1]^2/4\bar{n}_1\}} e^{-\{[\pm q(s-K)+u_2]^2/4\bar{n}_2\}} |
$$

$$
\times \bar{n}_1 + p(s+k) + u_1, \bar{n}_2 \pm q(s-k) + u_2\rangle_{\hat{H}}, \tag{21}
$$

with $L(s) = \max(-[2\sqrt{\bar{n}_1}/p] - s, -[2\sqrt{\bar{n}_2}/q] + s)$ and $U(s) = \min([2\sqrt{\bar{n}_1}/p] - s, [2\sqrt{\bar{n}_2}/q] + s)$. In general, the spatial properties of the state $|\Psi_{\bar{n}_1,\bar{n}_2}^{\pm p,q}(\gamma)\rangle_{s,u_1,u_2}$ weakly depend on the indices u_1 and u_2. The amplitude coefficients in Eq. (21) also reveal that the stationary coherent state $|\Psi_{\bar{n}_1,\bar{n}_2}^{\pm p,q}(\gamma)\rangle_{s,u_1,u_2}$ with index $s = 0$ has a dominant contribution in the wave-packet coherent state $|\Psi(t; \upsilon_1, \upsilon_2)\rangle$. For $s = u_1 = u_2 = 0$, the stationary coherent state $|\Psi_{\bar{n}_1,\bar{n}_2}^{\pm p,q}(\gamma)\rangle_{0,0,0}$ can be compactly expressed as

$$
|\Psi_{\bar{n}_1,\bar{n}_2}^{\pm p,q}(\gamma)\rangle_{0,0,0} = \frac{1}{\sqrt{2\pi\sqrt{\bar{n}_1\bar{n}_2}}} \sum_{k=-M}^{M}
$$

$$
\times e^{ik\gamma} e^{-[(pk)^2/4\bar{n}_1]} e^{-[(qk)^2/4\bar{n}_2]} |\bar{n}_1 + pk, \bar{n}_2 \mp qk\rangle_{\hat{H}}, \tag{22}
$$

where $M = \min([2\sqrt{\bar{n}_1}/p], [2\sqrt{\bar{n}_2}/q])$. The state $|\Psi_{\bar{n}_1,\bar{n}_2}^{\pm p,q}(\gamma)\rangle_{0,0,0}$ can be regarded as a representative state
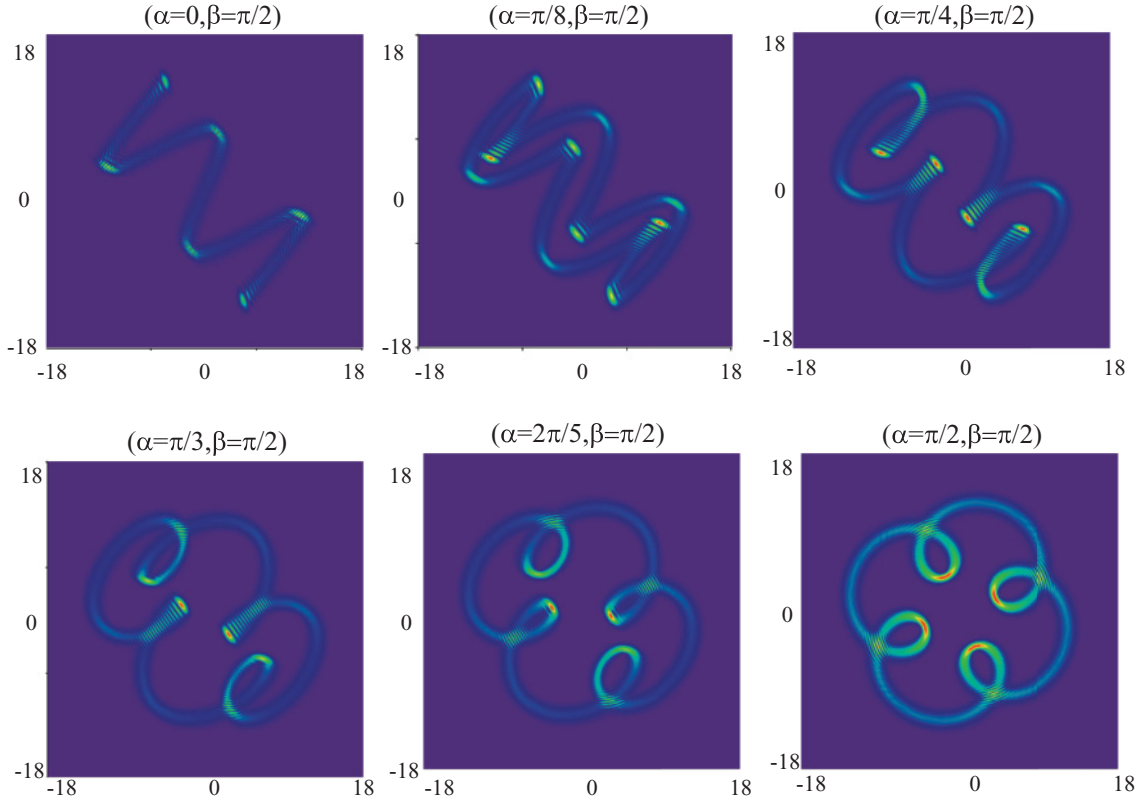
FIG. 4. (Color online) Wave patterns of the stationary coherent state $|\Psi_{\bar{n}_1,\bar{n}_2}^{\pm p,q}(\gamma)\rangle_{0,0,0}$ for the parameters corresponding to the classical orbits shown in Fig. 2.

that precisely mimics the spatial morphology of the time evolution of the wave-packet state $|\Psi(t;\upsilon_1,\upsilon_2)\rangle$.

Equation (22) was employed to calculate the wave patterns of the stationary coherent state $|\Psi_{\bar{n}_1,\bar{n}_2}^{\pm p,q}(\gamma)\rangle_{0,0,0}$ for the parameters corresponding to the classical orbits shown in Figs. 1 and 2. The calculated wave patterns are depicted in Fig. 3 for $(p,q)=(1,5)$ and in Fig. 4 for $(p,q)=(-1,5)$. It can be seen that the spatial morphologies of the stationary coherent state $|\Psi_{\bar{n}_1,\bar{n}_2}^{\pm p,q}(\gamma)\rangle_{0,0,0}$ are in excellent agreement with the Lissajous-trochoid transformed orbits. The agreement confirms the accuracy of the theoretical representation of the stationary coherent states related to the Lissajous-trochoid transformed orbits. Recently it has been experimentally realized in optics that various Lissajous coherent waves can be transformed into trochoidal coherent waves with cylindrical lenses to perform the SU(2) transformations [46–48]. Therefore, the present development of stationary coherent states is not only significant in understanding the quantum-classical connection to the SU(2) transformations but also useful in generating optical coherent waves based on the optical devices of mode converters.

V. CONCLUSION

In summary, the geometry of classical dynamics in the 2D coupled harmonic oscillator with SU(2) transformations has been investigated. It was found that the classical periodic orbits under SU(2) transformations are a family of continuous transformation orbits between Lissajous and trochoidal curves. The quantum wave-packet coherent states have been derived analytically to correspond exactly to the transformation geometry of classical dynamics. By using the quantum wave-packet coherent states derived herein, the stationary coherent states have been found to display the spatial morphologies related to the transformation geometries between Lissajous and trochoidal orbits. It is believed that the present investigation not only provides useful insight into the emerging field of quantum information technology but also paves the way for developing alternative [1] ideas in mathematical geometry.

[1] M. Brack, Rev. Mod. Phys. **65**, 677 (1993).

[2] W. A. De Heer, Rev. Mod. Phys. **65**, 611 (1993).

[3] I. V. Zozoulenko and K. F. Berggren, Phys. Rev. B **56**, 6931 (1997).

[4] R. Brunner, R. Meisels, F. Kuchar, R. Akis, D. K. Ferry, and J. P. Bird, Phys. Rev. Lett. **98**, 204101 (2007).

[5] A. D. Peters, C. Jaffé, and J. B. Delos, Phys. Rev. Lett. **73**, 2825 (1994).

[6] C. Bracher and J. B. Delos, Phys. Rev. Lett. **96**, 100404 (2006).

[7] E. Schrödinger, Naturwissenschaften **14**, 664 (1926).

[8] W. M. Zhang, D. H. Feng, and R. Gillmore, Rev. Mod. Phys. **62**, 867 (1990).

[9] W. H. Zurek, S. Habib, and J. P. Paz, Phys. Rev. Lett. **70**, 1187 (1993).

[10] J. A. Yeazell, M. Mallalieu, J. Parker, and C. R. Stroud, Phys. Rev. A **40**, 5040 (1989).

[11] C. Lena, D. Delande, and J. C. Gay, Europhys. Lett. **15**, 697 (1991).

[12] A. J. Makowski and K. J. Górska, J. Phys. A **40**, 11373 (2007).

[13] M. S. Kumar and B. Dutta-Roy, J. Phys. A **41**, 075306 (2008).

[14] K. F. Huang, Y. F. Chen, H. C. Lai, and Y. P. Lan, Phys. Rev. Lett. **89**, 224102 (2002).

[15] T. Gensty, K. Becker, I. Fischer, W. Elsäßer, C. Degen, P. Debernardi, and G. P. Bava, Phys. Rev. Lett. **94**, 233901 (2005).

[16] Y. F. Chen, K. W. Su, T. H. Lu, and K. F. Huang, Phys. Rev. Lett. **96**, 033905 (2006).

[17] E. J. Galvez, P. R. Crawford, H. I. Sztul, M. J. Pysher, P. J. Haglin, and R. E. Williams, Phys. Rev. Lett. **90**, 203901 (2003).

[18] I. Vorobeichik, E. Narevicius, G. Rosenblum, M. Orenstein, and N. Moiseyev, Phys. Rev. Lett. **90**, 176806 (2003).

[19] M. Brambilla, F. Battipede, L. A. Lugiato, V. Penna, F. Prati, C. Tamm, and C. O. Weiss, Phys. Rev. A **43**, 5090 (1991).

[20] D. Dangoisse, D. Hennequin, C. Lepers, E. Louvergneaux, and P. Glorieux, Phys. Rev. A **46**, 5955 (1992).

[21] E. Louvergneaux, D. Hennequin, D. Dangoisse, and P. Glorieux, Phys. Rev. A **53**, 4435 (1996).

[22] E. Louvergneaux, G. Slekys, D. Dangoisse, and P. Glorieux, Phys. Rev. A **57**, 4899 (1998).

[23] S. P. Hegarty, G. Huyet, J. G. McInerney, and K. D. Choquette, Phys. Rev. Lett. **82**, 1434 (1999).

[24] Y. F. Chen and Y. P. Lan, Phys. Rev. A **66**, 053812 (2002).

[25] F. Encinas-Sanz, S. Melle, and O. G. Calderón, Phys. Rev. Lett. **93**, 213904 (2004).

[26] E. Cabrera, O. G. Calderón, S. Melle, and J. M. Guerra, Phys. Rev. A **73**, 053820 (2006).

[27] G. P. Karman, G. S. McDonald, G. H. C. New, and J. P. Woerdman, Nature (London) **402**, 138 (1999).

[28] Y. F. Chen, Y. P. Lan, and K. F. Huang, Phys. Rev. A **68**, 043803 (2003).

[29] Y. F. Chen, T. H. Lu, K. W. Su, and K. F. Huang, Phys. Rev. E **72**, 056210 (2005).

[30] Y. F. Chen, T. H. Lu, K. W. Su, and K. F. Huang, Phys. Rev. Lett. **96**, 213902 (2006).

[31] T. H. Lu, Y. C. Lin, Y. F. Chen, and K. F. Huang, Phys. Rev. Lett. **101**, 233901 (2008).

[32] V. Bužek and T. Quang, J. Opt. Soc. Am. B **6**, 2447 (1989).

[33] J. Banerji and G. S. Agarwal, Opt. Express **5**, 220 (1999).

[34] G S Agarwal and J Banerji, J. Phys. A: Math. Nucl. Gen. **39**, 11503 (2006).

[35] R. G. Nazmitdinov, Phys. Part. Nucl. **40**, 71 (2009).

[36] B. L. Johnson and G. Kirczenow, Europhys. Lett. **51**, 367 (2000).

[37] P. K. Bhaduri, S. Li, K. Tanaka, and J. C. Waddington, J. Phys. A: Math. Nucl. Gen. **27**, L553 (1994).

[38] W. D. Heiss and R. G. Nazmitdinov, Phys. Rev. Lett. **73**, 1235 (1994).

[39] J. Schwinger, in *Quantum Theory of Angular Momentum*, edited by L. C. Biedenharn and H. van Dam (Academic, New York, 1965), pp. 229–279.

[40] M. S. Kim, W. Son, V. Bužek, and P. L. Knight, Phys. Rev. A **65**, 032323 (2002).

[41] B. C. Sanders, K. S. Lee, and M. S. Kim, Phys. Rev. A **52**, 735 (1995).

[42] W. Louisell, *Radiation and Noise in Quantum Electronics* (McGraw-Hill, New York, 1964), p. 274.

[43] D. J. Wineland, C. Monroe, W. M. Itano, B. E. King, D. Leibfried, C. Myatt, and C. Wood, Phys. Scr. T **76**, 147 (1998).

[44] S. J. M. Habraken and G. Nienhuis, Phys. Rev. A **75**, 033819 (2007).

[45] G. S. Agarwal, J. Opt. Soc. Am. A **16**, 2914 (1999).

[46] Y. F. Chen, Y. C. Lin, K. F. Huang, and T. H. Lu, Phys. Rev. A **82**, 043801 (2010).

[47] E. G. Abramochkin and V. G. Volostnikov, J. Opt. A **6**, S157 (2004).

[48] L. E. Vicent and K. B. Wolf, J. Opt. Soc. Am. A **25**, 1875 (2008).